ELSEVIER

Journal of Computational and Applied Mathematics 93 (1998) 123–143

JOURNAL OF COMPUTATIONAL AND APPLIED MATHEMATICS

A numerical method to compute the dissolution of second phases in ternary alloys

Fred Vermolen[a], Kees Vuik[b,*]

[a] *Laboratory of Materials Science, Delft University of Technology, P.O. Box 5045, NL 2600 GA Delft, Netherlands*
[b] *Faculty of Technical Mathematics and Informatics, Delft University of Technology, P.O. Box 5031, NL 2600 GA Delft, Netherlands*

Received 12 December 1997; received in revised form 21 April 1998

Abstract

Dissolution of stoichiometric multi-component particles in ternary alloys is an important process occurring during the heat treatment of as-cast aluminium alloys prior to hot extrusion. A mathematical model is proposed to describe such a process. In this model an equation is given to determine the position of the particle interface in time, using two diffusion equations which are coupled by nonlinear boundary conditions at the interface. Some results concerning existence, uniqueness, and monotonicity are given. Furthermore, for an unbounded domain an analytical approximation is derived. The main part of this work is the development of a numerical solution method. Finite differences are used on a grid which changes in time. The discretization of the boundary conditions is important to obtain an accurate solution. The resulting nonlinear algebraic system is solved by the Newton–Raphson method. Numerical experiments illustrate the accuracy of the numerical method. The numerical solution is compared with the analytical approximation.

AMS classification: 35R35; 65M06; 80A22

Keywords: Stefan problem; Moving grid method; Stoichiometric particle dissolution; Ternary alloy homogenisation

1. Introduction

Heat treatment of metals is often necessary to optimise their mechanical properties both for further processing and for final use. During the heat treatment the metallurgical state of the alloy changes. This change can either involve the phases being present or the morphology of the various phases. Whereas the equilibrium phases can be predicted quite accurately from the thermodynamic models, there are no general models for microstructural changes nor general models for the kinetics of these changes. In the latter cases both the initial morphology and the transformation mechanisms have to

* E-mail: c.vuik@math.tudelft.nl.

0377-0427/98/$19.00
PII S0377-0427(98)00076-4

be specified explicitly. One of these processes that is amenable to modelling is the dissolution of second phase particles in a matrix with a uniform initial composition.

To describe this particle dissolution in solid media several physical models for binary alloys have been developed, incorporating the effects of long-distance diffusion [35, 3, 28] and nonequilibrium conditions at the interface [20, 1, 29]. These articles did not cover the technologically important dissolution of stoichiometric multi-component particles in ternary alloys.

The phase transformation element in steel has been studied in [12, 33]. Reiso [23] investigated the dissolution of Mg_2Si-particles in aluminium alloys mainly experimentally. He compared his results to a simple dissolution model valid for dissolution in infinite media. All analyses indicate that the addition of a second alloying element can influence the dissolution kinetics strongly. However, in none of these articles attention was paid to the effect of the particle geometry on the dissolution of particles in ternary alloys. The present article describes the dissolution of spherical and needle-shaped particles, a planar medium, a spherical layer of segregation and the combination of a dissolving particle and a dissolving spherical layer of segregation. In many metallurgical situations, the thermal treatment also aims at the dissolution of the segregation layer around the grains. In the articles mentioned, no attention was paid to the impact of all physical parameters on the overall dissolution kinetics.

The present work covers a detailed numerical analysis of a coupled Stefan problem in which two boundaries either move or are fixed. The diffusion equation is solved using a finite difference discretization. The displacement of the boundary is computed with a front-tracking method. The concentration of both chemical elements are linked via the hyperbolic relation between the Dirichlet conditions corresponding to both diffusing elements. The disappearance of a moving boundary is incorporated and modelled by a transition of a Dirichlet condition to a Neumann condition. The calculation can then be continued until complete homogenisation has been reached. We expect that our approach is applicable to a much wider class of Stefan problems involving more equations or other coupling conditions. This is a point of current research.

The mathematical model for the dissolution of second phases in ternary alloys is given in Section 2. Some remarks about existence, uniqueness and properties of the solution are given in Section 3. In Section 4 the numerical method is specified. Some properties of the numerical method are investigated in Section 5. In this section also a number of metallurgical applications are solved and properties of their solutions are given.

2. A model of dissolution in ternary alloys

Consider three chemical species denoted by A, B, and C. We investigate the dissolution of an $A_lB_mC_n$ particle in an A–B–C alloy, where we assume that the concentrations of B and C are small with respect to that of component A. The concentrations of B and C are written as c_B, c_C (mol/m^3), respectively. At a given temperature the initial concentrations are equal to c_B^0 and c_C^0. The concentrations of B and C in the particle are denoted by $c_{B,\mathrm{part}}$ and $c_{C,\mathrm{part}}$. The interface concentrations ($c_{B,\mathrm{sol}}$ and $c_{C,\mathrm{sol}}$) are variant.

We consider a one-dimensional problem. The geometry is given by $\Omega(t) = \{x \in \mathbb{R} \mid M_1 \leqslant S_1(t) \leqslant x \leqslant S_2(t) \leqslant M_2\}$, $t \in [0, T]$ where T is an arbitrary positive number. In some applications there is a time t_1 and t_2 such that, respectively, $S_1(t) = M_1, t \geqslant t_1$ and $S_2(t) = M_2, t \geqslant t_2$. For the determination

of c_B, c_C we use the multi-component version of Fick's second law (see [30, 21] [p. 160]):

$$\frac{\partial c_p}{\partial t} = \frac{1}{r^a}\frac{\partial}{\partial r}\left(\mathbb{D}_{p,B} r^a \frac{\partial c_B}{\partial r}\right) + \frac{1}{r^a}\frac{\partial}{\partial r}\left(\mathbb{D}_{p,C} r^a \frac{\partial c_C}{\partial r}\right), \quad r \in \Omega(t),\ t \in (0,T],\ p \in \{B,C\}, \tag{1}$$

where a is a geometric parameter, which equals 0,1, or 2 for, respectively, a planar, a cylindrical, or a spherical geometry. Note that M_1 should be nonnegative for $a \neq 0$. All these geometries occur in metallurgical applications. For simplicity, we assume $\mathbb{D}_{B,C} = \mathbb{D}_{C,B} = 0$, both species diffuse independently, and that $\mathbb{D}_{B,B} = \mathbb{D}_B, \mathbb{D}_{C,C} = \mathbb{D}_C$ (m^2/s) are constant. Hence, the equations given in Eq. (1) reduce to

$$\frac{\partial c_p}{\partial t} = \frac{\mathbb{D}_p}{r^a}\frac{\partial}{\partial r}\left(r^a \frac{\partial c_p}{\partial r}\right), \quad r \in \Omega(t),\ t \in (0,T],\ p \in \{B,C\}. \tag{2}$$

As initial conditions we use

$$c_p(r,0) = c_p^0(r), \quad r \in \Omega(0),\ p \in \{B,C\}, \tag{3}$$

where c_p^0 are given nonnegative functions. When a moving boundary becomes fixed, i.e., $S_k(t) = M_k$, we assume that there is no flux through the boundary, so

$$\frac{\partial c_p}{\partial r}(M_k,t) = 0 \quad \text{for } t \geqslant t_k,\ p \in \{B,C\},\ k \in \{1,2\}. \tag{4}$$

On the moving boundaries a Dirichlet boundary condition is used:

$$c_p(S_k(t),t) = c_{p,k,sol}(t), \quad t \in [0,T],\ p \in \{B,C\},\ k \in \{1,2\}. \tag{5}$$

So, six unknown quantities remain: $S_k(t), c_{B,k,sol}(t)$, and $c_{C,k,sol}(t)$, $k \in \{1,2\}$. To obtain a unique solution six boundary conditions are necessary. We assume that the particle is stoichiometric, which means that $c_{A,part}, c_{B,part}$, and $c_{C,part}$ are constant. Using the Gibbs free energy of the stoichiometric compound we get [30]

$$(c_{B,k,sol}(t))^m \cdot (c_{C,k,sol}(t))^n = K, \quad k \in \{1,2\}, \tag{6}$$

where the exponents m,n correspond to the stoichiometric phase $A_l B_m C_n$ and K is a constant depending on temperature. The balance of B and C atoms and the constant composition of the particle lead to the following equations [24] for the moving boundary positions:

$$(c_{p,part} - c_{p,k,sol}(t))\frac{dS_k}{dt}(t) = \mathbb{D}_p \frac{\partial c_p}{\partial r}(S_k(t),t), \quad t \in (0,T],\ p \in \{B,C\},\ k \in \{1,2\}. \tag{7}$$

Condition (7) implies

$$\frac{\mathbb{D}_B}{c_{B,part} - c_{B,k,sol}(t)}\frac{\partial c_B}{\partial r}(S_k(t),t) = \frac{\mathbb{D}_C}{c_{C,part} - c_{C,k,sol}(t)}\frac{\partial c_C}{\partial r}(S_k(t),t), \quad k \in \{1,2\}. \tag{8}$$

The moving boundary problem given by Eqs. (2)–(7) is known as a Stefan problem. For a recent book where this type of problems is considered we refer to [32] (see, for instance, p. 132, (2.5),(2.9)). There are some differences between the dissolution in a binary alloy [30] and in a ternary alloy. In the first place, two diffusion equations have to be solved, which are coupled through the conditions (5)–(7) on the moving boundaries. Secondly, the problems are nonlinear due to the balance of atoms on S_1, S_2, both in the binary and the ternary case. However, in the mathematical model for a ternary alloy an extra nonlinearity occurs in Eq. (6). Survey papers and books on the Stefan problem are [9, 16, 8, 17, 5, 25].

3. Properties of the Stefan problem

After the description of a maximum principle we give some results concerning existence, uniqueness, and monotonicity of solutions of the given Stefan problem. Also an approximate solution is given for the dissolution of a particle in an unbounded domain ($M_2 = \infty$).

3.1. The maximum principle for the diffusion equation

First a few basic principles are formulated, which are used later in this section. The Stefan problem is formed by the diffusion equation and a displacement equation for one or more moving boundaries. For the diffusion equation it can be proved that the solution satisfies a maximum principle, which we present for completeness.

Maximum principle:

Suppose c satisfies the inequality

$$\frac{\partial^2 c}{\partial r^2} - \frac{\partial c}{\partial t} \geqslant 0, \quad r \in \Omega(t), \ t \in (0, T], \tag{9}$$

then a local maximum has to occur at one or both of the sides S_1, S_2 (the moving boundaries), or at $t = 0$ (the initial condition). Suppose that a local maximum occurs at the point P on S_1, or S_2. If $\partial/\partial v$ denotes the derivative in an outward direction from $\Omega(t)$, then $\partial c/\partial v > 0$ at P.

This statement is referred to as the maximum principle and has been proved by Protter and Weinberger for a general parabolic operator (see [22] [p.168,170]). This principle can also be applied for local minima (and $\partial c/\partial v < 0$) when the inequality in Eq. (9) is reversed. The principle thus requires the global extremes of a solution to the diffusion equation to occur either at the boundaries S_1, S_2, or at $t = 0$.

3.2. Some limitations of the Stefan problem

In this section we consider some artificial problems, in order to investigate the limitations of our mathematical model. In the first example we show that the model breaks down when the concentration at the interface is equal to the particle concentration. From the second example it appears that difficulties occur when the initial concentration is equal to the particle concentration. Then the ternary model should be replaced by a binary model.

The movement of the boundaries S_1, S_2 is given by Eq. (7). This holds provided $c_{p,\mathrm{sol}} \neq c_{p,\mathrm{part}}$, $p \in \{\mathrm{B}, \mathrm{C}\}$ to prevent a division by zero. If $(\partial c_p/\partial r)(S_k(t), t) \neq 0$ then a division by zero would imply an infinite displacement. Such a situation can occur, for example, when we have an initial concentration profile in which $c_p^0(r) < c_{p,\mathrm{part}}$ for $r \in (S_1(0), (S_1(0) + S2(0))/2)$ and $c_p^0(r) > c_{p,\mathrm{part}}$ for $r \in ((S_1(0) + S2(0))/2, S_2(0))$. Simulations have shown that then possibly $c_{p,\mathrm{sol}}$ converges to $c_{p,\mathrm{part}}$, causing a division by zero when computing the displacement of the boundary. These examples shows that in general it is impossible to show global existence of the solution. A blow up in finite time is possible. This kind of problems have been a popular topic in recent free boundary research [14, 31, 26, 27, 37, 38, 2, 13]. However, in our metallurgical applications we never encounter this type of problem, because the initial concentrations are always less than the concentrations in the particle. For cylindrical and spherical problems blow up occurs when the particle disappears. From a practical point of view the effect of this blow up on the concentration profiles is negligible.

We consider the following planar problem: $c_{\mathrm{C}}^0 = 0$, $c_{\mathrm{B}}^0 = c_{\mathrm{B,part}}$, $S_2(t) = M_2$, and for simplicity Eq. (4) is replaced by

$$c_p(M_2, t) = c_p^0, \quad p \in \{\mathrm{B}, \mathrm{C}\}. \tag{10}$$

Suppose that S_1, c_{B}, and c_{C} are a solution of the Stefan problem, where $0 \leqslant c_{\mathrm{C,sol}}(t) \leqslant c_{\mathrm{C,part}}$. Then we have the following result:

Proposition. *There is no $\hat{t} > 0$ such that $S_1(t)$ is monotone on $[0, \hat{t}]$, unless $c_{\mathrm{B,sol}}(t) = c_{\mathrm{B,part}}$.*

Proof. Suppose there is a $\hat{t} > 0$ such that $\mathrm{d}S_1/\mathrm{d}t \geqslant 0, t \in [0, \hat{t}]$. This assumption together with the inequality $c_{\mathrm{C,sol}}(t) \leqslant c_{\mathrm{C,part}}$, and Eq. (7) implies that $(\partial c_{\mathrm{C}}/\partial r)(S_1(t), t) \geqslant 0$, $t \in [0, \hat{t}]$. Eq. (6) implies that $c_{\mathrm{C,sol}}(t) \neq 0$. From the maximum principle it follows that the maximum occurs at S_1. However, at such a point the inequality $(\partial c_{\mathrm{C}}/\partial r)(S_1(t), t) < 0$ holds. This leads to a contradiction.

Now we assume that there is a $\hat{t} > 0$ such that $\mathrm{d}S_1/\mathrm{d}t \leqslant 0$, $t \in [0, \hat{t}]$. When there is a $\tilde{t} \in [0, \hat{t}]$ such that $c_{\mathrm{B,sol}}(\tilde{t}) > c_{\mathrm{B,part}}$, Eq. (7) implies that $(\partial c_{\mathrm{C}}/\partial r)(S_1(\tilde{t}), \tilde{t}) \geqslant 0$. Using the maximum principle as before, we again obtain a contradiction. In the same way it can be proved that $c_{\mathrm{B,sol}}(\tilde{t}) < c_{\mathrm{B,part}}$ is impossible. □

This proposition implies that the only physically acceptable solution occurs when $c_{\mathrm{B,sol}}(t) = c_{\mathrm{B,part}}$. In this case we are faced with a division by zero when computing the displacement of the boundary. However, due to the maximum principle $c_{\mathrm{B}}(r, t) = c_{\mathrm{B,part}} = c_{\mathrm{B}}^0$, so $(\partial c_{\mathrm{B}}/\partial r)(S_1(t), t) = 0$. Hence, we are faced with a zero-by-zero division. From a thermodynamic point of view it is reasonable that for this case there is no change of the concentration profile in the matrix. The boundary conditions are coupled via Eq. (6). The solution for this situation can be obtained using the solution of the concentration profile of the element C only. We are thus faced with a binary diffusion problem, in which the interfacial concentration of element C is then determined by the concentration of element B by Eq. (6).

3.3. Monotonicity properties

Consider the solution of the Stefan problem: S_1, c_{B}, and c_{C}, where $S_2 = M_2$ and Eq. (4) replaced by Eq. (10). We assume that $c_{\mathrm{B}}^0 < c_{\mathrm{B,part}}$. Suppose that at some time, t_1, $c_{\mathrm{B}}(S_1(t_1), t_1) < c_{\mathrm{B,part}}$ and at a

later time, $t_3 > t_1$, we would have $c_B(S_1(t_3), t_3) > c_{B,part}$. From the continuity of $c_B(S_1(t), t)$, it follows that for some time, t_2, such that $t_1 < t_2 < t_3$, $c_B(S_1(t), t) < c_{B,part}$, $t \in [t_1, t_2)$, and $c_B(S_1(t_2), t_2) = c_{B,part}$. According to Eq. (7), $(\partial c_B/\partial r)(S_1(t_2), t_2) = 0$. This violates the maximum principle. A similar situation can be analysed for $c_B^0 > c_{B,part}$, and $c_B(S_1(t_1), t_1) > c_{B,part}$. From this it can be concluded that the sign of $c_p(S_k(t), t) - c_{p,part}$ does not change with time, provided this sign is equal to the sign of $c_p^0(r) - c_{p,part}$ for all r.

3.4. An approximate solution

For the classical one-phase planar Stefan problem ($M_1 = -\infty$, $M_2 = 0$, $c^0 = 1$, $c(S(t), t) = 0$, $\lambda \mathrm{d}S/\mathrm{d}t = -(\partial c/\partial r)(S(t), t)$) a self-similar solution is already found by Neumann in 1860 [34] [p.122]: $S(t) = k\sqrt{t}$ and $c(x,t) = 1 - (1 + \mathrm{erf}(x/2\sqrt{t}))/(1 + \mathrm{erf}(k/2))$, where k satisfies the transcendental equation

$$k = \frac{2}{\lambda\sqrt{\pi}} \frac{\exp(-(k/2)^2)}{1 + \mathrm{erf}(k/2)}.$$

Our approximate solution is related to a self-similar solution as given above.

For the case that diffusion takes place in an infinite medium with spherical symmetry near a spherical particle, the Laplace transform can be used to solve the problem. The diffusion equation for spherical symmetry determines the transport of matter:

$$\frac{\partial c_p}{\partial t} = \frac{\mathbb{D}_p}{r^2} \frac{\partial}{\partial r} \left(r^2 \frac{\partial c_p}{\partial r} \right), \quad p \in \{\mathrm{B}, \mathrm{C}\}.$$

The condition at the interface is given by

$$c_p(S_1(t), t) = c_{p,sol}(t).$$

At infinity and for $t = 0$:

$$c_p(r, 0) = c_p^0, \quad c_p(\infty, t) = c_p^0,$$

where c_p^0 are given constants. We approximate the function $c_{p,sol}(t)$ by a constant value $\hat{c}_{p,sol}$. By means of the (inverse) Laplace transform an approximate solution [35] is given by

$$\tilde{c}_p(r,t) = c_p^0 + (\hat{c}_{p,sol} - c_p^0) * \frac{S_1(t)}{r} * \mathrm{Erfc}\left(\frac{r - S_1(t)}{2\sqrt{\mathbb{D}_p t}} \right). \tag{11}$$

This approximation is exact when $S_1(t)$ is constant. So we assume that the difference between the exact solution and the approximation is small as long as $S_1(t)$ is a slowly varying function. Substitution of $\tilde{c}_p$ into Eq. (7), yields

$$\frac{\mathrm{d}S_1(t)}{\mathrm{d}t} = -\frac{\hat{c}_{p,sol} - c_p^0}{c_{p,part} - c_{p,sol}} \left(\frac{\mathbb{D}_p}{S_1(t)} + \sqrt{\frac{\mathbb{D}_p}{\pi t}} \right). \tag{12}$$

Combination of both components to fullfill the requirement as stated by Eq. (8), it follows that

$$\frac{\hat{c}_{\mathrm{B,sol}} - c^0_{\mathrm{B}}}{c_{\mathrm{B,part}} - \hat{c}_{\mathrm{B,sol}}} \left(\frac{\mathbb{D}_{\mathrm{B}}}{S_1(t)} + \sqrt{\frac{\mathbb{D}_{\mathrm{B}}}{\pi t}} \right) = \frac{\hat{c}_{\mathrm{C,sol}} - c^0_{\mathrm{C}}}{c_{\mathrm{C,part}} - \hat{c}_{\mathrm{C,sol}}} \left(\frac{\mathbb{D}_{\mathrm{C}}}{S_1(t)} + \sqrt{\frac{\mathbb{D}_{\mathrm{C}}}{\pi t}} \right). \tag{13}$$

Using Eq. (6) as the relation between the concentrations at the interface S_1, it follows that for $t \downarrow 0$:

$$\frac{\hat{c}_{\mathrm{B,sol}} - c^0_{\mathrm{B}}}{c_{\mathrm{B,part}} - \hat{c}_{\mathrm{B,sol}}} * \sqrt{\frac{\mathbb{D}_{\mathrm{B}}}{\mathbb{D}_{\mathrm{C}}}} = \frac{(K/\hat{c}^n_{\mathrm{B,sol}})^{1/m} - c^0_{\mathrm{C}}}{c_{\mathrm{C,part}} - (K/\hat{c}^n_{\mathrm{B,sol}})^{1/m}}. \tag{14}$$

As has been remarked before, it has been assumed that the interfacial concentration is constant in time. The variation of the interfacial concentration with time is most significant at the early stages: the interfacial concentrations then change from c^0_p to $\hat{c}_{p,\mathrm{sol}}$. In the later stages, the interfacial concentrations will vary less with time and the above used approximation may be more accurate. As the diffusion of the chemical elements proceeds, the elements reach the other boundary. Then, an accumulation of atoms occurs there. However, this analytical model does not incorporate this effect since it is assumed that the domain in which the elements diffuse is infinite. Therefore, at the later stages this approximation will become less accurate as well.

For the case of a particle stoichiometry BC, i.e. $n = m$, the following quadratic equation results from Eq. (14): $\alpha(\hat{c}_{\mathrm{B,sol}})^2 + \beta\hat{c}_{\mathrm{B,sol}} + \gamma = 0$ with α, β, γ given as

$$\alpha = c_{\mathrm{C,part}} - \sigma c^0_{\mathrm{C}}, \quad \beta = \sigma c_{\mathrm{B,part}} c^0_{\mathrm{C}} - c^0_{\mathrm{B}} c_{\mathrm{C,part}} + K(\sigma - 1), \quad \gamma = (c^0_{\mathrm{B}} - \sigma c_{\mathrm{B,part}})K,$$

where $\sigma = \sqrt{\mathbb{D}_{\mathrm{C}}/\mathbb{D}_{\mathrm{B}}}$. If $(\sigma c^0_{\mathrm{C}} - c_{\mathrm{C,part}})(\sigma c_{\mathrm{B,part}} - c^0_{\mathrm{B}}) < 0$ then there is only one root for which the inequality $\hat{c}_{\mathrm{B,sol}} > 0$ holds. If however, $(\sigma c^0_{\mathrm{C}} - c_{\mathrm{C,part}})(\sigma c_{\mathrm{B,part}} - c^0_{\mathrm{B}}) > 0$ and the discriminant is positive then we have to keep in mind that the roots have to meet the requirement that the Stefan problem is not degenerate, i.e., we may not have $0 \leqslant c^0_p < c_{p,\mathrm{part}} < c_{p,\mathrm{sol}}$ or $0 < c_{p,\mathrm{sol}} < c_{p,\mathrm{part}} < c^0_p$, $p \in \{\mathrm{B}, \mathrm{C}\}$. A root that does not satisfy this requirement is rejected. It appears that indeed two nonnegative, nondegenerate solutions for $\hat{c}_{\mathrm{B,sol}}$ can be obtained.

Consider the following example: $(c_{\mathrm{B,part}}, c_{\mathrm{C,part}}) = (50, 1)$, $(c^0_{\mathrm{B}}, c^0_{\mathrm{C}}) = (2, 30)$, $\mathbb{D}_{\mathrm{C}} = 2 * \mathbb{D}_{\mathrm{B}} = 2 \cdot 10^{-13}\,\mathrm{m}^2/\mathrm{s}$, and the value of K is varied. The interface concentrations have been calculated and substituted in Eq. (12) to obtain the interface velocity for $t \downarrow 0$. The interface velocity coefficient $\mathrm{d}S(t)/\mathrm{d}t \cdot \sqrt{t}$ is plotted in Fig. 1. For $0 < K < 50$, it can be seen that the discriminant is positive and hence two solutions are obtained. One of the solutions is degenerate and is therefore rejected. The other one leads to a positive boundary velocity so the particle increases. For $50 < K < 470.33$ two nondegenerate solutions exist. Both solutions have a negative boundary velocity so the particle dissolves. For $K = 470.33$ the discriminant is zero and the solutions coincide. Considering the discriminant of the quadratic equation, it follows that the discriminant is negative for $470.33 < K < 55681$ giving two complex solutions. The solutions for $K > 55681$ are both degenerate. It appeared from numerical experiments that the slower solution is more stable numerically. It appears that this stability depends on the formulation of the zero-point problem. For higher orders (different stoichiometries) it is very hard to state any general remarks about the solution.

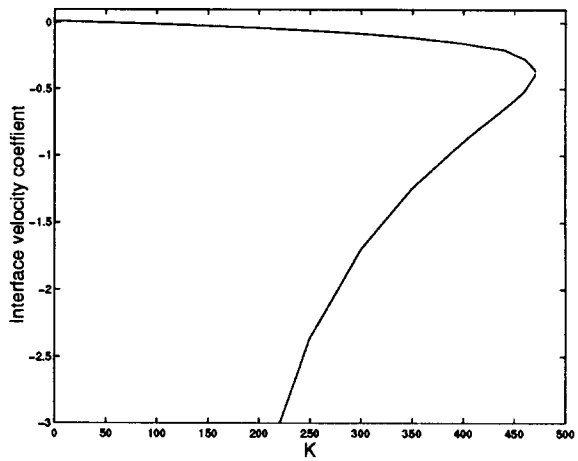

Fig. 1. Interface velocity for various values of K.

4. The numerical method

Various numerical methods are known to solve Stefan problems. In [9] the following types of method are distinguished: front-tracking, front-fixing, and fixed-domain methods. In a front-fixing method a transformation of coordinates is used (a special case is the isotherm migration method (IMM)). Fixed domain methods are the enthalpy method (EM) and the variational inequality method (VI). Various methods are compared in [10]. The latter methods (IMM, EM, VI) are only applicable when the concentration is constant at the interface. Since in our problem the concentration varies at the interface we restrict ourselves to a front-tracking method. Front-tracking methods are described in [19, 4, 15, 36, 39]. Our main interest is to give an accurate discretization of the boundary conditions. Therefore, we use the classical moving grid method of Murray and Landis [19] to discretize the diffusion equations. First an outline of the numerical method is given. Thereafter each part is described in more detail.

The equations are solved with a finite difference method in the r and t-direction. A characteristic feature of a front-tracking method is that the interface positions are nodal points in every time-step. So, the position of the grid points depends on time. An outline of the algorithm is:

(1) Compute the concentration profiles solving the nonlinear problem given by Eqs. (2)–(6) and (8).
(2) Predict the positions of S_1 and S_2 at the new time-step: $S_1(t+\Delta t)$ and $S_2(t+\Delta t)$.
(3) Redistribute the grid such that $S_1(t+\Delta t)$ and $S_2(t+\Delta t)$ are nodal points.
(4) Return to step 1.

We introduce the following notation: the time-step is $\Delta t = T/N_T$, and the positions of the interfaces are denoted by $S_k^j = S_k(j\Delta t)$, $k \in \{1,2\}$. The step-size in the space direction is $\Delta r^j = (S_2^j - S_1^j)/N$, and $r_i^j = S_1^j + i\Delta r^j$, $i \in \{0,\ldots,N\}$. In some expressions $r_{i\pm1/2}^j$ is used, which is equal to $S_1^j + (i\pm\frac{1}{2})\Delta r^j$. Finally, the concentration $c_k(r_i^j, j\Delta t)$ is approximated by $c_{k,i}^j$, $k \in \{\mathrm{B},\mathrm{C}\}$. In the remainder of this section we give a detailed description of the various parts of our algorithm. In this paper we explain the method for an equidistant grid. In practice one can save much computation time when the grid is refined in the neighbourhood of the moving boundaries.

4.1. Discretization of the interior region

In this section we use the symbols c and $\mathbb{D}$ instead of $c_B, c_C, \mathbb{D}_B$, or $\mathbb{D}_C$. We suppose that S_k^{j+1} and c_i^j are given. The concentration on the new time-step satisfies the following equation:

$$\frac{c_i^{j+1}}{\mathbb{D}\Delta t} + \{[(r_{i+1/2}^{j+1})^a + (r_{i-1/2}^{j+1})^a]c_i^{j+1} - (r_{i-1/2}^{j+1})^a c_{i-1}^{j+1} - (r_{i+1/2}^{j+1})^a c_{i+1}^{j+1}\}/\{(r_i^{j+1})^a(\Delta r^{j+1})^2\}$$

$$= \frac{1}{\mathbb{D}\Delta t}\left\{c_i^j + \frac{c_{i+1}^j - c_{i-1}^j}{2\Delta r^j}(r_i^{j+1} - r_i^j)\right\}, \quad i = 1,\ldots,N-1. \tag{15}$$

In this formula central differences are used to discretize the term $(1/r^a)(\partial/\partial r)(r^a \partial c/\partial r)$. The final term is caused by the changing mesh. The value of c_i^j is given in the point $(r_i^j, j\Delta t)$. However, for the time derivative it is necessary to evaluate c_i^j at $(r_i^{j+1}, j\Delta t)$. Linear interpolation is used to approximate this value:

$$c_i^j(r_i^{j+1}, j\Delta t) \simeq c_i^j + \left(\frac{\partial c}{\partial r}\right)_i^j (r_i^{j+1} - r_i^j) \simeq c_i^j + \frac{c_{i+1}^j - c_{i-1}^j}{2\Delta r^j}(r_i^{j+1} - r_i^j).$$

For $a > 0$ a division by zero could occur in Eq. (15) when $r_i^{j+1} = 0$. Since $i \geqslant 1$ and $S_1^j \geqslant M_1 \geqslant 0$, the value of r_i^{j+1} is always positive, so Eq. (15) is valid also for $a > 0$.

4.2. Discrete boundary condition at a fixed boundary

At a fixed boundary the Neumann boundary condition (4) holds. For a discrete version of this condition we assume that Eq. (15) is also valid for $i = 0$, and $i = N$. Note that virtual concentrations c_{-1}^{j+1}, and c_{N+1}^{j+1} occur. These concentrations are eliminated by using the discrete analogue of Eq. (4):

$$\frac{c_1^{j+1} - c_{-1}^{j+1}}{2\Delta r^{j+1}} = 0, \quad \frac{c_{N+1}^{j+1} - c_{N-1}^{j+1}}{2\Delta r^{j+1}} = 0. \tag{16}$$

An exception is made for the case $i = 0$, and $a > 0$, because then Eq. (15) contains a division by zero. Now Eq. (4) is replaced by a balance of atoms. For $a = 2$ the balance is considered for a sphere with radius $\frac{1}{2}\Delta r^{j+1}$:

$$\frac{c_0^{j+1} - c_0^j}{\Delta t}\frac{4\pi}{3}\left(\frac{\Delta r^{j+1}}{2}\right)^3 = \mathbb{D}4\pi\left(\frac{\Delta r^{j+1}}{2}\right)^2 \frac{c_1^{j+1} - c_0^{j+1}}{\Delta r^{j+1}}.$$

Using cylinder coordinates a similar expression holds. After simplification for spherical and cylindrical geometry the resulting equations are

$$\frac{c_0^{j+1} - c_0^j}{\Delta t}\frac{\Delta r^{j+1}}{2(a+1)} = \mathbb{D}\frac{c_1^{j+1} - c_0^{j+1}}{\Delta r^{j+1}}, \quad a \in \{1,2\}. \tag{17}$$

4.3. Discrete boundary condition at a moving boundary

In the numerical method we assume that the positions of the boundaries are known at $t^{j+1} = (j+1)\Delta t$. Hence, on each boundary (S_1, S_2) two boundary conditions (6), (8) are necessary. The

derivatives used in Eq. (8) are discretized with central differences including the virtual concentrations c_{-1}^{j+1}, and c_{N+1}^{j+1}. We assume again that Eq. (15) holds for $i=0$, and $i=N$. Condition (6) is replaced by

$$(c_{\mathrm{B},0}^{j+1})^m(c_{\mathrm{C},0}^{j+1})^n = K, \qquad (c_{\mathrm{B},N}^{j+1})^m(c_{\mathrm{C},N}^{j+1})^n = K. \tag{18}$$

Summarising, we note that at the new time-step $2(N+3)$ unknowns are used, whereas up to now only $2(N+2)$ equations are specified. This implies that the solution consists of a two-parameter family. To determine a unique solution we assume that all concentrations are a function of $c_{\mathrm{B},0}^{j+1}$, and $c_{\mathrm{B},N}^{j+1}$. These remaining unknowns are determined by the following coupled nonlinear equations (cf. (8)):

$$f_1(c_{\mathrm{B},0}^{j+1}, c_{\mathrm{B},N}^{j+1}) \equiv \mathbb{D}_{\mathrm{B}}(c_{\mathrm{C,part}} - c_{\mathrm{C},0}^{j+1})(c_{\mathrm{B},1}^{j+1} - c_{\mathrm{B},-1}^{j+1}) - \mathbb{D}_{\mathrm{C}}(c_{\mathrm{B,part}} - c_{\mathrm{B},0}^{j+1})(c_{\mathrm{C},1}^{j+1} - c_{\mathrm{C},-1}^{j+1}) = 0 \tag{19}$$

and

$$\begin{aligned} f_2(c_{\mathrm{B},0}^{j+1}, c_{\mathrm{B},N}^{j+1}) \equiv{}& \mathbb{D}_{\mathrm{B}}(c_{\mathrm{C,part}} - c_{\mathrm{C},N}^{j+1})(c_{\mathrm{B},N+1}^{j+1} - c_{\mathrm{B},N-1}^{j+1}) \\ &- \mathbb{D}_{\mathrm{C}}(c_{\mathrm{B,part}} - c_{\mathrm{B},N}^{j+1})(c_{\mathrm{C},N+1}^{j+1} - c_{\mathrm{C},N-1}^{j+1}) = 0. \end{aligned} \tag{20}$$

So the problem has been reduced to obtaining a root for the vector function (f_1, f_2). We approximate this root by the Newton–Raphson method.

The pth iterates of the concentrations are denoted by $c_{\mathrm{B},i}^{j+1}(p)$, $i \in \{0,N\}$. The continuous Newton–Raphson method runs as follows:

$$\begin{pmatrix} c_{\mathrm{B},0}^{j+1}(p+1) \\ c_{\mathrm{B},N}^{j+1}(p+1) \end{pmatrix} = \begin{pmatrix} c_{\mathrm{B},0}^{j+1}(p) \\ c_{\mathrm{B},N}^{j+1}(p) \end{pmatrix} + (J(p))^{-1} \begin{pmatrix} -f_1(p) \\ -f_2(p) \end{pmatrix}, \tag{21}$$

where J is the Jacobian. In practice, it is impossible to compute J, so we use a discrete approximation $\hat{J}$. The elements of the 2×2 matrix $\hat{J}$ are

$$\begin{aligned} \hat{J}_{k,i} = {}& [f_k(c_{\mathrm{B},0}^{j+1} + (2-i)\varepsilon, c_{\mathrm{B},N}^{j+1} + (i-1)\varepsilon) - f_k(c_{\mathrm{B},0}^{j+1} - (2-i)\varepsilon, c_{\mathrm{B},N}^{j+1} \\ & -(i-1)\varepsilon)]/2\varepsilon, \quad k,i \in \{1,2\}. \end{aligned}$$

The discretization of the Jacobian is determined using a central difference in order to guarantee an accuracy of $O(\varepsilon^2)$. From a numerical point of view it is important to note that ε has to be sufficiently small, but larger than the accuracy of the numerical scheme to evaluate the concentrations.

To start the Newton–Raphson procedure an initial guess has to be found. To prevent convergence to an undesired root, the initial guess is chosen as close as possible to the root. For time-steps $j>1$, the boundary concentrations from the former time-step are chosen as initial guesses. However, at time step $j=1$, the roots of (see Eq. (14))

$$\frac{x - c_{\mathrm{B}}^0(r_i)}{c_{\mathrm{B,part}} - x}\sqrt{\frac{\mathbb{D}_{\mathrm{B}}}{\mathbb{D}_{\mathrm{C}}}} = \frac{\sqrt[m]{K/x^n} - c_{\mathrm{C}}^0(r_i)}{c_{\mathrm{C,part}} - \sqrt[m]{K/x^n}}, \quad i \in \{0,N\} \tag{22}$$

are used. We terminate the iteration when

$$|c_{\mathrm{B},0}^{j+1}(p+1) - c_{\mathrm{B},0}^{j+1}(p)| + |c_{\mathrm{B},N}^{j+1}(p+1) - c_{\mathrm{B},N}^{j+1}(p)| < \varepsilon.$$

The given approach is adapted for the case $a>0$ and $S_1^{j+1}<\Delta r^{j+1}$. In this case the virtual grid-point near S_1 is released. The derivatives in Eq. (8) are replaced by one-sided differences, and Eq. (15) is no longer used for $i=0$. When an accurate solution is needed at this point of blow up, a numerical method based on the phase field model [6, 7] can be used.

4.4. Adaptation of the moving boundaries

We have only used one-half of the boundary conditions given in Eq. (7) to determine the concentrations. The remaining conditions are used to adapt the positions of the moving boundaries. The adaptation of S_1 and S_2 is comparable, therefore we only describe the determination of S_1. Two different methods are described.

An Euler forward time integration yields

$$S_1^{j+1}=S_1^j+\frac{\mathbb{D}_B\Delta t}{c_{B,\text{part}}-c_{B,0}^j}\frac{c_{B,1}^j-c_{B,-1}^j}{2\Delta r^j},\quad S_2^{j+1}\ \text{idem.}$$

Due to the explicit nature of this adaptation it is important to choose the time-step not too large relative to the grid-size. In our computations we choose Δt such that $\Delta t\leqslant 10(\Delta r^0)^2/\max\{\mathbb{D}_B,\mathbb{D}_C\}$. The virtual concentrations $c_{B,-1}^j, c_{B,N+1}^j$, are computed from Eq. (15). For $a>0$ and $S_1^j<\Delta r^{j+1}$ the central finite difference to approximate $(\partial c_B/\partial r)(S_1(t),t)$ is replaced by a one-sided finite difference, as has been mentioned in the previous section. When the distance between a moving boundary and a fixed boundary is small $((S_k^{j+1}-M_k)/(S_k^0-M_k)<\varepsilon,\ k\in\{1,2\})$ we fix the boundary $(S_k^{j+1}=M_k,\ k\in\{1,2\})$, and change the boundary conditions accordingly.

The second method is the Trapezium method. Since this method is implicit the new positions of the moving boundaries are computed iteratively (cf. [15]). The outline of the algorithm is summarised as follows:

(1) $p:=0$ (p is the iteration number).

(2) $c_{B,i}^{j+1}(p)=c_{B,i}^j,\ i\in\{0,N\}$.

(3) $S_1^{j+1}(p)=S_1^j+\frac{\mathbb{D}_B\Delta t}{c_{B,\text{part}}-c_{B,0}^j}\frac{c_{B,1}^j-c_{B,-1}^j}{2\Delta r^j}$, $S_2^{j+1}(p)$ idem (predictor).

(4) Generate mesh, i.e., determine $r_i^{j+1}(p)$.

(5) Carry out one Newton–Raphson iteration step (Eq. (21)) and solve the diffusion equation to obtain $c_{B,i}^{j+1}(p+1)$ and $c_{C,i}^{j+1}(p+1)$.

(6) $S_1^{j+1}(p+1)=S_1^j+\frac{\mathbb{D}_B\Delta t}{2}\{\frac{c_{B,1}^j-c_{B,-1}^j}{2\Delta r^j(c_{B,\text{part}}-c_{B,0}^j)}+\frac{c_{B,1}^{j+1}(p+1)-c_{B,-1}^{j+1}(p+1)}{2\Delta r^{j+1}(p)(c_{B,\text{part}}-c_{B,0}^{j+1}(p+1))}\}, S_2^{j+1}(p+1)$ idem (corrector).

(7) While
$|c_{B,0}^{j+1}(p+1)-c_{B,0}^{j+1}(p)|+|c_{B,N}^{j+1}(p+1)-c_{B,N}^{j+1}(p)|+\frac{|S_1^{j+1}(p+1)-S_1^{j+1}(p)|}{|S_1^j-M_1|}+\frac{|S_2^{j+1}(p+1)-S_2^{j+1}(p)|}{|S_2^j-M_2|}>\varepsilon\ p:=p+1$
go to step 4.

(8) $c_{B,i}^{j+1}=c_{B,i}^{j+1}(p)$, $c_{C,i}^{j+1}=c_{C,i}^{j+1}(p)$, and $S_k^{j+1}=S_k^{j+1}(p)$, $k\in\{1,2\}$, do next time iteration.

Using the above algorithm the accuracy of the free boundary position is improved. The roots of the vector function (f_1,f_2) are determined within the same iteration as the free boundary positions S_1^{j+1} and S_2^{j+1}. Since in step 5 of the algorithm only one Newton–Raphson iteration step is performed, the order of the total amount of work done at each time-step is similar to the order of the total amount of work done at one Euler forward iteration.

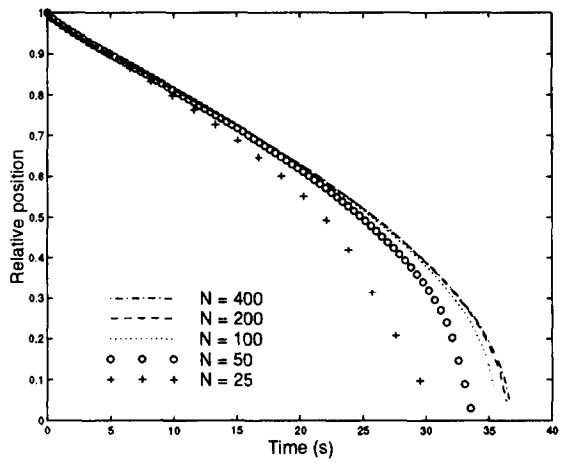

Fig. 2. Relative position of the interface $S_1(t)/S_1(0)$; with a virtual point.

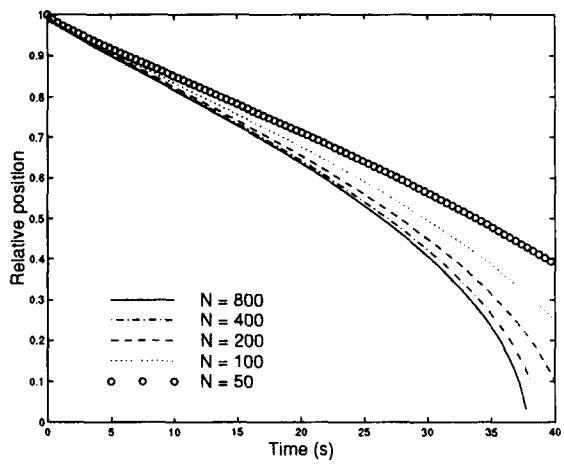

Fig. 3. Relative position of the interface $S_1(t)/S_1(0)$; without a virtual point.

5. Numerical experiments

In all computations the position of the interfaces are determined with the Euler forward method, except in the section where the Euler forward and the Trapezium method are compared.

5.1. The accuracy of the space discretization

In order to determine the accuracy of the calculations, grid-size and time-step dependence tests have been carried out. The results are shown in Figs. 2and 3. The following input parameters have been used: $\mathbb{D}_C = 2$ $\mathbb{D}_B = 2 \cdot 10^{-13}\,\mathrm{m}^2/\mathrm{s}$, $c_p^0 = 0, c_{p,\mathrm{part}} = 50$, $p \in \{B, C\}, K = 1$, $m = n = 1$, $S_1(0) = 5 \cdot 10^{-7}\,\mathrm{m}$, $M_2 = 5 \cdot 10^{-6}\,\mathrm{m}$, $S_2(0) = M_2$, and we assume spherical geometry. The grid-size and time-step were decreased until the differences are negligible for the whole simulation. It can be seen in Figs. 2 and 3 that the distances between all curves are negligible for small times. For larger

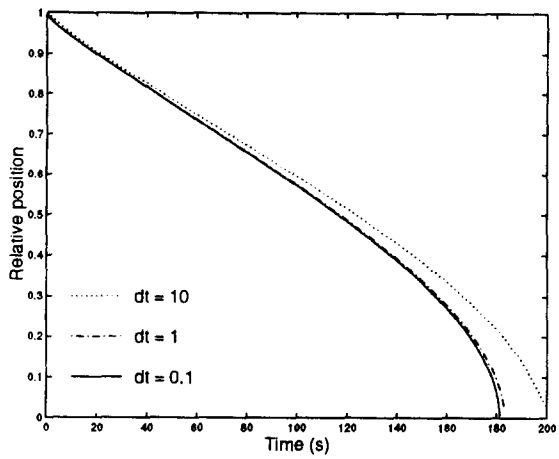

Fig. 4. Relative position of the interface $S_1(t)/S_1(0)$; with the Euler forward method.

times the differences increase. The use of a virtual point at the interface increases the accuracy considerably. The observed rate is $O(\Delta r^2)$ with a virtual point and $O(\Delta r)$ without a virtual point.

In case of the use of a virtual grid point, the central discretization reads as follows:

$$\frac{c_{p,1}^j - c_{p,-1}^j}{2\Delta r^j} = \frac{\partial c_p}{\partial r}(S_1(t_j), t_j) + \frac{(\Delta r^j)^2}{6}\frac{\partial^3 c_p}{\partial r^3}(\theta_1, t_j), \quad \theta_1 \in (S_1(t_j) - \Delta r^j,\ S_1(t_j) + \Delta r^j).$$

Without the use of a virtual grid point we have the following one-sided discretization:

$$\frac{c_{p,1}^j - c_{p,0}^j}{\Delta r^j} = \frac{\partial c_p}{\partial r}(S_1(t_j), t_j) + \frac{\Delta r^j}{2}\frac{\partial^2 c_p}{\partial r^2}(\theta_2, t_j), \quad \theta_2 \in (S_1(t_j), S_1(t_j) + \Delta r^j).$$

In the vicinity of the interface we observe the following inequalities: $\partial c_p/\partial r < 0, \partial^2 c_p/\partial r^2 > 0$, $\partial^3 c_p/\partial r^3 < 0$. Therefore, in case of the presence of a virtual grid point and without a virtual grid point, respectively, the discretization at the interface overestimates (Fig. 2) respectively underestimates (Fig. 3) the interface velocity.

5.2. The accuracy of the time integration

We used the same input-parameters for the determination of the accuracy of the time integration except for $S_1(0) = 10^{-6}$ m. The time-step was varied until convergence was reached. The results have been printed in Fig. 4 (Euler Forward) and Fig. 5 (Trapezium). It can be well observed that the difference between the two methods is small as long as the time-step is sufficiently small ($\Delta t \leqslant 1$ s, corresponding to $\Delta t \leqslant 312.5(\Delta r^0)^2/\max\{\mathbb{D}_B, \mathbb{D}_C\}$). The results obtained with the Euler forward method become inaccurate when $\Delta t \geqslant 10$ s, whereas the Trapezium method still produces accurate results.

5.3. A comparison of the analytical and numerical solution

As has been mentioned before, the initial guess for the interfacial concentrations is based on some analytical considerations. The derivation of this analytical approximation is summarised in

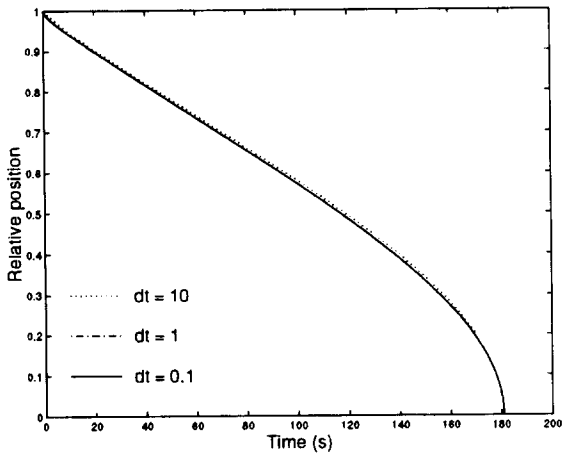

Fig. 5. Relative position of the interface $S_1(t)/S_1(0)$; with the Trapezium method.

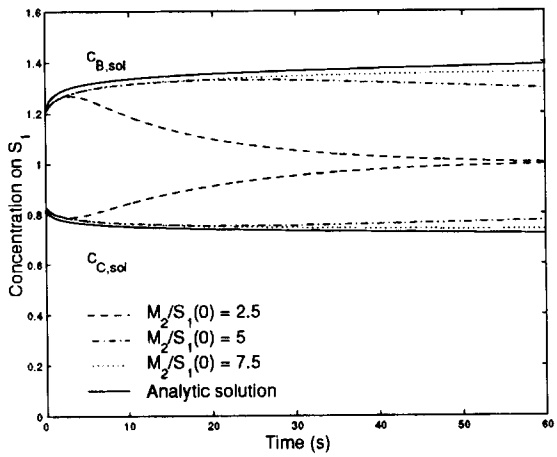

Fig. 6. Interface concentrations for various values of $M_2/S_1(0)$.

Section 3. This expression holds for spherical symmetry, but it can be used for planar geometry as well [1]. Unfortunately, this derivation has to be done under the assumption that the interfacial concentration remains constant during the entire dissolution process. At the early stages of the dissolution process, the interfacial concentration does not remain constant (see Fig. 6). To compute the interfacial concentration we iterate the analytical solution using the following predictor-corrector method with a sufficiently small time-step:

Predictor-corrector method:

(1) Compute $\hat{c}_{B,sol}(\Delta t)$ from Eq. (14), $j=1$.

(2) Substitute $\hat{c}_{B,sol}(\Delta t)$ in Eq. (12) and compute $S_1(j\cdot\Delta t)$.

(3) Using $S_1(j\cdot\Delta t)$, obtain $c_{B,sol}((j+1)\cdot\Delta t)$ from Eqs. (8) and (13), $j:=j+1$, go to 2.

The results obtained with the analytic approach are of the same order of magnitude as the results obtained using the finite difference scheme (see Fig. 6). The finite difference results in Fig. 6 have been obtained using various $M_2/S_1(0)$-values. Though there is a small difference between the results from the analytical and numerical scheme already at early stages, it can be seen that for large $M_2/S_1(0)$-values the match between the analytical approximation and the numerical solution is good. This is as expected, because the analytical approximation is based on the dissolution of a spherical particle in an infinite medium. The differences at early stages are due to the rather large variation of the Dirichlet conditions with time. At later stages, the Dirichlet conditions vary less with time and the difference between the results stops increasing. An advantage of the analytical approximation is that it costs a negligible amount of CPU-time. However, in reality the effects of soft-impingement (a bounded domain) are relevant. Then the analytical approximation is not reliable.

5.4. An analysis of the discretized Jacobian

In subsection 4.3 the Newton–Raphson procedure to obtain the Dirichlet conditions has been outlined. In this method the Jacobian plays an important role. The Jacobian consists of the derivatives of both boundary functions f_i, $i \in \{1,2\}$, with respect to $c_{\mathrm{B,sol}}$ at both boundaries. Therefore, during each zero point iteration we determine f_1, f_2 at $(c_{\mathrm{B,sol}}(S_1), c_{\mathrm{B,sol}}(S_2))$, $(c_{\mathrm{B,sol}}(S_1) \pm \varepsilon, c_{\mathrm{B,sol}}(S_2))$, and $(c_{\mathrm{B,sol}}(S_1), c_{\mathrm{B,sol}}(S_2) \pm \varepsilon)$, which means that in every iteration the discretized equations have to be solved 5 times. It is obvious that for the case that the diffusion fields between the boundaries S_1 and S_2 do not interact, the off-diagonal coefficients of the Jacobian are negligible and could be set zero. In this case it is sufficient to evaluate f_1, f_2 at $(c_{\mathrm{B,sol}}(S_1), c_{\mathrm{B,sol}}(S_2))$, $(c_{\mathrm{B,sol}}(S_1) + \varepsilon, c_{\mathrm{B,sol}}(S_2) + \varepsilon)$, and $(c_{\mathrm{B,sol}}(S_1) - \varepsilon, c_{\mathrm{B,sol}}(S_2) - \varepsilon)$, so the discretized equations need only be solved 3 times, which speeds up the calculation. For each time-step, about 4 Newton–Raphson iterations had to be applied to get the desired accuracy.

The off-diagonal Jacobian terms have been analysed relative to the diagonal Jacobian terms (i.e., $J_{1,2}/J_{1,1}$ and $J_{2,1}/J_{2,2}$). It appeared that these values remained approximately constant during an entire simulation, also when the diffusion fields of both phases started to impinge. In Fig. 7 the off-diagonal Jacobian terms have been displayed as a function of the dimensionless time-step defined by: $\alpha = \sqrt{\min(\mathbb{D}_B, \mathbb{D}_C) * \Delta t}/(S_2(0) - S_1(0))$. It can be seen that the influence of the cross-terms in the Jacobian increases with increasing time-step. This may be explained using the theory of penetration. It can be proved that for a planar medium the penetration depth as a function of time is given by $L(t) = \sqrt{\pi \max(\mathbb{D}_B, \mathbb{D}_C)t}$. The penetration depth corresponds to the minimal distance from one of the moving boundaries to the position where the concentration has been unchanged. For the ternary case, the interfacial concentrations change during each time-step Δt. If $L(\Delta t) \lesssim S_2(0) - S_1(0)$ then the changes of the interfacial concentrations do not influence each other, i.e., the off-diagonal terms of the Jacobian are negligible.

For the planar geometry, we have by symmetry $J_{1,2}/J_{1,1} = J_{2,1}/J_{2,2}$. In the cylindrical and spherical cases we have the inequality $J_{1,2}/J_{1,1} > J_{2,1}/J_{2,2}$. This inequality becomes stronger for the spherical case. The inequality will be explained for the spherical geometry. As the area of S_2 is larger than the area of S_1 and the area increases from S_1 to S_2, the influence on the boundary condition at S_1 by the boundary condition at S_2 will be larger than the influence on the boundary condition at S_2 by the boundary condition at S_1. Therefore we have the inequality $J_{1,2}/J_{1,1} > J_{2,1}/J_{2,2}$. A similar explanation may be given for the case of cylindrical geometry.

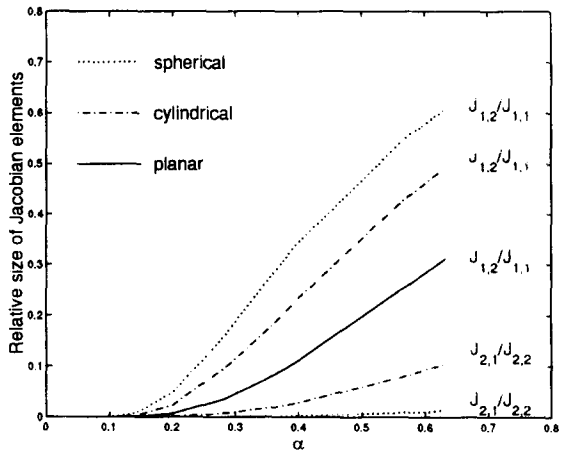

Fig. 7. Relative size of the Jacobian elements.

For the planar geometry, the penetration depth may be written as

$$L(\Delta t)=\sqrt{\pi\max(\mathbb{D}_B,\mathbb{D}_C)\,\Delta t}=\sqrt{\frac{\pi\max(\mathbb{D}_B,\mathbb{D}_C)}{\min(\mathbb{D}_B,\mathbb{D}_C)}}\alpha(S_2(0)-S_1(0)).$$

From this it follows that

$$\alpha=\sqrt{\frac{\min(\mathbb{D}_B,\mathbb{D}_C)}{\pi\max(\mathbb{D}_B,\mathbb{D}_C)}}\,\frac{L(\Delta t)}{S_2(0)-S_1(0)}$$

is an important dimensionless number. From Fig. 7 it can be seen that if $\alpha < 0.1$ the off-diagonal terms of the Jacobian are negligible for all geometries.

5.5. *Application to the movement of two boundaries in a ternary alloy*

Some calculations for a ternary alloy have been carried out with two simultaneously moving boundaries. Fig. 8 shows some results for the boundary position as a function of time. The input parameters for these curves are $\mathbb{D}_C=2\mathbb{D}_B=2\cdot 10^{-13}\,m^2/s$, $c_p^0=0, c_{p,\text{part}}=50$, $p\in\{B,C\}$, $K=1$, $m=n=1, S_1(0)=7.5\cdot10^{-7}\,m$, $M_2=5\cdot10^{-6}\,m$, $M_2-S_2(0)=2\cdot10^{-8}\,m$, $N=500, \Delta t=100\Delta r^2/\max(\mathbb{D}_B,\mathbb{D}_C)$.

It can be seen in Fig. 8 that the dissolution time is largest for a spherical segregation layer (S_2). For both cylindrical and spherical geometries the surface of the segregation layer increases during the dissolution process. For the particle (S_1) it takes most time to dissolve for the planar geometry, as the surface of the particle decreases during dissolution for both cylindrical and spherical geometry. For a comparison the curve of S_1, without the presence of S_2, versus time has been displayed for a spherical geometry. It appears that the dissolution of a particle is considerably delayed by the presence of a segregation layer. It can be observed as well that at the early stages there is no influence on the dissolution kinetics of S_1 from the boundary S_2.

To illustrate the behaviour of the concentration profile, the concentration profiles of both chemical elements at different times have been presented in Fig. 9 for the spherical geometry. As is to be

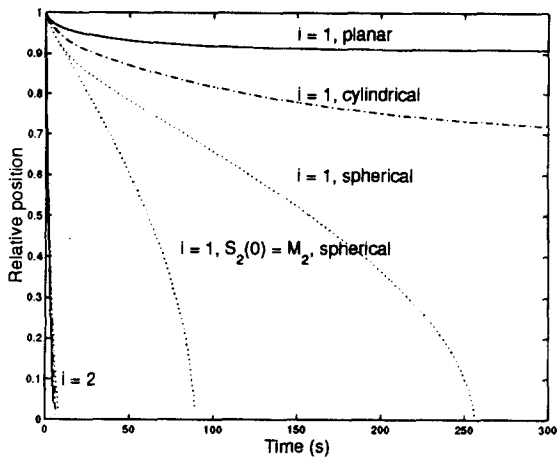

Fig. 8. Relative position of the interfaces $(S_i(t) - M_i)/((S_i(0) - M_i)$.

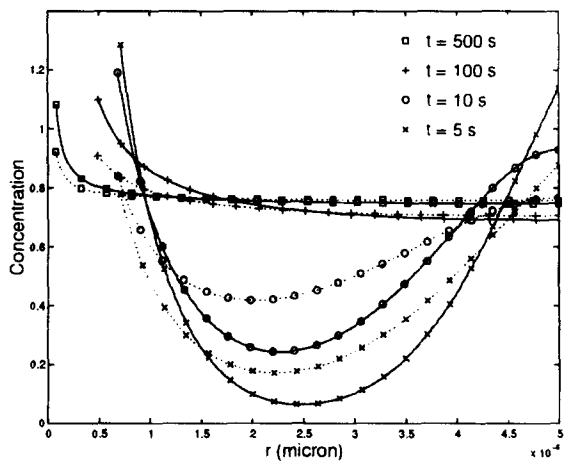

Fig. 9. The concentrations for a spherical geometry (— $c_B, \ldots c_C$).

expected, at the early stages the profiles are very steep. The interfacial concentrations at S_1 converge during dissolution as a result of soft-impingement. For the concentration profile at $t = 5$ s, Dirichlet conditions are in effect at both boundaries: both S_1 and S_2 are moving. For $t = 10$ s it can be seen that the boundary condition at S_2 has changed into a Neumann condition: no mass transfer is allowed through the boundary. Later, when $S_1 = M_1$ (dissolution of the particle) a Neumann condition is applied at S_1 too. Finally the profile becomes homogeneous.

5.6. *The influence of the diffusion coefficients of both elements*

To illustrate the applicability of the model, some calculations have been carried out for the case of a stoichiometric spherical second phase Mg_2Si and Mg_2X in a ternary aluminium alloy. The diffusion coefficients $\mathbb{D}_{Si}$ and $\mathbb{D}_{Mg}$, taken from Fujikawa [11] and Yamane [18] for a temperature of 793 K, are $2.15 \cdot 10^{-13}$ and $3.24 \cdot 10^{-13}$ m^2/s, respectively. Furthermore, the initial particle radius, the

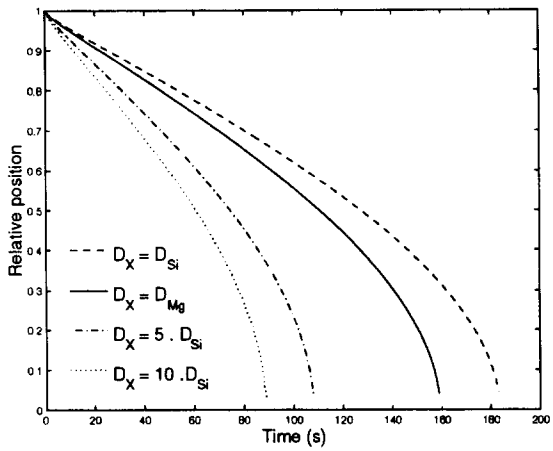

Fig. 10. Relative position of the interface $S_1(t)/S_1(0)$.

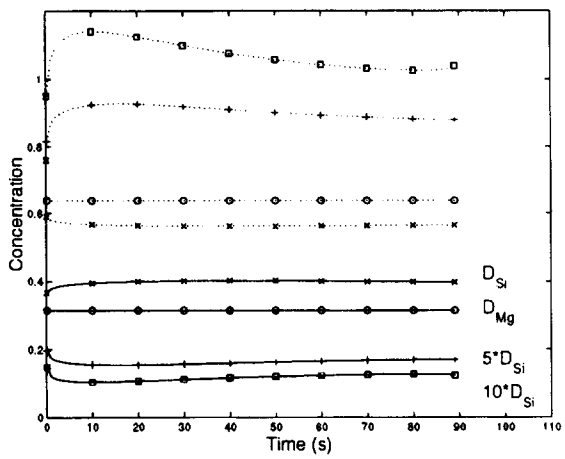

Fig. 11. Concentration at the interface (— $c_X, \ldots c_{Mg}$).

cell radius, and initial matrix concentrations have been taken, respectively, as 10^{-6} m, $8\cdot10^{-6}$ m, 0, 0. For K the value of 0.35 has been used. As the calculation concerns an Mg_2X particle, we have $c_{Mg,part} = 66.7\%$.

In Fig. 10 the interfacial position for the case of dissolution of a spherical Mg_2X particle in aluminium is given. Various choices for the diffusion coefficient $\mathbb{D}_X$ are used. The special choice $\mathbb{D}_X = \mathbb{D}_{Mg}$ corresponds to the dissolution of an Mg particle, so this is a binary alloy. Note that initially the interfacial velocity decreases. At the final stages of dissolution, the interfacial area has become so small, that the interfacial velocity has to be large to satisfy the Stefan condition. It can be seen from Fig. 10 that the addition of a second element can influence the dissolution kinetics strongly.

Fig. 11 represents the interfacial concentration at S_1 of both alloying elements as a function of time. From Fig. 11 it is clear that at the initial stages the atoms of the slower element accumulate

near the interface. On the other hand, the atoms of the faster element diffuse deeper into the matrix. This causes the diverging behaviour of the interfacial concentrations at early stages.

A more detailed analysis in which the stoichiometry, cell size and diffusion coefficient have been varied can be found in [30].

6. Conclusions

A mathematical model is given to describe the dissolution of stoichiometric multi-component particles in ternary alloys. Some results concerning existence and uniqueness are given.

An analytical approximate solution is given, valid when the dissolution takes place in an unbounded domain. The results are cheap to calculate and they are reasonably accurate. This analytical approximation can also be used for short simulation times in a bounded domain, or as starting solution for the Newton–Raphson process used in the numerical method.

The numerical method described is second order accurate when virtual points are used to discretize the boundary conditions at the interface. The Trapezium method to compute the interface positions is more accurate than the Euler forward method, whereas the computational costs per iteration are comparable. A criterion is given to estimate when the off-diagonal terms of the Jacobian are negligible. Then the computational work can be decreased considerably. The numerical solutions lead to valuable insight for metallurgical applications.

A number of open questions remain:

- Is the model valid when blow up occurs?
- Which numerical method should be used to compute a solution which blows up?
- A point of current research is an extension of the described model to alloys with more chemical elements.
- The analytical approximation suggests that for some choices of parameters the problem has more than one solution. Further research is needed at this point, especially when different stoichiometries ($n \neq m$) are used.

Acknowledgements

The authors thank Prof.dr.ir. P. Wesseling for carefully reading the manuscript and giving advice to improve it, and one of the referees whose valuable suggestions improve the manuscript considerably.

References

[1] H.B. Aaron, G.R. Kotler, Second phase dissolution, Metall. Trans. 2 (1971) 393–407.

[2] T. Aiki, Behavior of free boundaries of blow-up solutions to one-phase Stefan problems, Nonlinear Anal. 26 (1996) 707–723.

[3] U.L. Baty, R.A. Tanzilli, R.W. Heckel, Dissolution kinetics of CuAl2 in an Al–4Cu alloy, Metall. Trans. 1 (1970) 1651–1656.

[4] R. Bonnerot, P. Jamet, A second order finite element method for the one-dimensional Stefan problem, Int. J. Num. Meth. Engng 8 (1974) 811–820.

[5] M. Brokate, N. Kenmochi, I. Müller, J.F. Rodriguez, C. Verdi, Phase transitions and hysteresis; lectures given at the 3rd session of the Centro Internazionale Matematico Estivo (CIME) held in Montecatini Terme, Italy, July 13–21, 1993, Lecture notes in mathematics 1584, Springer, Berlin, 1994.
[6] G. Caginalp, An analysis of a phase field model of a free boundary, Arch. Rat. Mech. Anal. 92 (1986) 205–245.
[7] G. Caginalp, J.T. Lin, A numerical analysis of an anisotropic phase field model, IMA J. Appl. Math. 39 (1987) 51–66.
[8] J. Chadam, H. Rasmussen, Free Boundary Problems Involving Solids, Longman, Scientific & Technical Harlow, 1993.
[9] J. Crank, Free and Moving Boundary Problems, Clarendon Press, Oxford, 1984.
[10] A.J. Dalhuijsen, A. Segal, Comparison of finite element techniques for solidification problems, Int. J. Num. Meth. Engng. 23 (1986) 1807–1829.
[11] S. Fujikawa, K. Hirano, Y. Fujikawa, Diffusion of Silicon in Aluminium, Metall. Trans. A 9A (1978) 1811–1815.
[12] J. Ågren, Diffusion in phases with several components and sublattices, J. Phys. Chem. Solids 43 (1981) 421–430.
[13] Z. Guan, X. Wang, Existence and blow-up of solutions to two-phase nonequilibrium problems, SIAM J. Math. Anal. 27 (1996) 1038–1048.
[14] D. Howison, J.R. Ockendon, A.A. Lacey, Singularity development in moving boundary problems, Quart. J. Mech. Appl. Math. 38 (1985) 343–360.
[15] P. Lesaint, R. Touzani, Approximation of the heat equation in a variable domain with application to the Stefan problem, SIAM J. Numer. Anal. 26 (1989) 366–379.
[16] E. Magenes, C. Verdi, A. Visintin, Theoretical and numerical results on the two-phase Stefan problem, SIAM J. Numer. Anal. 26 (1989) 1425–1438.
[17] A.M. Meirmanov, The Stefan problem, De Gruyter Expositions in Mathematics, vol. 3, Walter de Gruyter, Berlin, 1992.
[18] Y. Minamino, T. Yamane, A. Shimomura, M. Shimada, M. Koizumi, N. Ogawa, J. Takahashi, H. Kimura, Effect of high pressure on interdiffusion in an Al–Mg alloy, J. Mater. Sci. 18 (1983) 2679–2687.
[19] W.D. Murray, F. Landis, Numerical and machine solutions of transient heat-conduction problems involving melting or freezing, Trans. ASME (C) J. Heat Transfer 81 (1959) 106–112.
[20] F.V. Nolfi Jr., P.G. Shewmon, J.S. Foster, The dissolution and growth kinetics of spherical precipitates, Trans. Metall. Soc. AIME 245 (1969) 1427–1433.
[21] R.L. Parker, Crystal growth mechanisms: energetics, kinetics and transport, Solid State Phys. 25 (1970) 152–298.
[22] M.H. Protter, H.F. Weinberger, Maximum Principles in Differential Equations, Prentice-Hall, Englewood Cliffs, 1967.
[23] O. Reiso, N. Ryum, J. Strid, Melting and dissolution of secondary phase particles in AlMgSi-alloys, Metall. Trans. A 24A (1993) 2629–2641.
[24] G. Segal, K. Vuik, F. Vermolen, A conserving discretization for the free boundary in a two-dimensional Stefan problem, Report 97-13, Faculty of Technical Mathematics and Informatics, Delft University of Technology, Delft, 1997.
[25] J.A. Sethian, Level Set Methods; Evolving Interfaces in Geometry, Fluid Mechanics, Computer Vision, and Materials Science, Cambridge monographs on applied and computational mathematics 3, Cambridge University Press, Cambridge, 1996.
[26] A. Solomon, A. Alexiades, D.G. Wilson, The initial velocity of the emerging free boundary in a two phase Stefan problem with imposed flux, SIAM J. Math. Anal. 18 (1987) 1438–1452.
[27] J.M. Sullivan, D.R. Lynch, Non linear simulation of dendritic solidification of an undercooled melt, Int. J. Numer. Meth. Engng. 25 (1988) 415–444.
[28] U.H. Tundal, N. Ryum, Dissolution of particles in binary alloys: Part I. computer simulations, Metall. Trans. 23A (1992) 433–449.
[29] F.J. Vermolen, S. Van der Zwaag, A numerical model for the dissolution of spherical particles in binary alloys under mixed mode control, Mater. Sci. Engng. A 220 (1996) 140–146.
[30] F. Vermolen, K. Vuik, S. van der Zwaag, The dissolution of a stoichiometric second phase in ternary alloys: a numerical study, Mater. Sci. Engng. A 246 (1998) 93–103.
[31] A. Visintin, A new model for supercooling and superheating effects, I.M.A. J. Appl. Math. 36 (1986) 141–157.
[32] A. Visintin, Models of Phase Transitions, Progress in Nonlinear Differential Equations and Their Application: 28, Birkhäuser, Boston, 1996

[33] J.M. Vitek, S.A. Vitek, S.A. David, Modelling of diffusion controlled phase transformation in ternary systems and application to the Ferrite/Austenite transformation in the Fe-Cr-Ni-system, Metall. Trans. A 26A (1995) 2007–2025.
[34] H. Weber, Die partiellen Differential-Gleichungen de mathematischen Physik II, Vieweg, Braunschweig, 1901.
[35] M.J. Whelan, On the kinetics of particle dissolution, Met. Sci. J. 3 (1969) 95–97.
[36] D.E. Womble, A front-tracking method for multiphase free boundary problems, SIAM J. Numer. Anal. 26 (1989) 380–396.
[37] W.Q. Xie, The Stefan problem with a kinetic condition at the free boundary, SIAM J. Math. Anal. 21 (1990) 362–373.
[38] H. Yin, Blowup and global existence for a non-equilibrium phase change process, in: A. Friedman, J. Spruck (Eds.), Variational and free boundary problems, The IMA volumes in mathematics and its application, vol. 53, Springer, New York, 1993, pp. 195–204.
[39] M. Zerroukat, C.R. Chatwin, Computational moving boundary problems, Appl. Engng. Math. ser. 8, Wiley, New York, 1994.